4th International Conference on Molten Slags and Fluxes, 1992, Sendai, ISIJ

THE MECHANISM OF SULPHUR MOVEMENT INTO THE MOLTEN SLAG PHASE FROM LIQUID STEEL

Tarek El Gammal, Buong-Mo Lim and Erwin Wosch

Dept. of Steelmaking, Aachen University of Technology (RWTH)

Aachen, F. R. GERMANY

Synopsis: The mechanism of sulphur transport from the steel bath to slag droplets produced by slag injection processes has been investigated by simulation experiments.Powdered slags were introduced onto the surface of small steel melts and the ensuing sulphur and iron profiles were determined by microprobe analysis. The results show that there is a clear difference in the mode of sulphur (and iron) transport between acid and basic slags due to the differing transport mechanisms. A critical radius for suspended slag droplets in relation to sulphur pick-up with time has been calculated, based on the experimental data.

Key words: slag droplets, sulphur pick-up, transport mechanisms, concentration profiles, slag basicity, initial sulphur concentration, critical slag droplet size.

1. Introduction

The injection of slag mixtures, based mostly on the $CaO-Al_2O_3-SiO_2$ system, to desulphurize the steel bath is well-established practice in ladle metallurgy. The efficiency of such treatment depends not only on the reactivity of the slag droplets, but also on the speed with which the reacting and reacted species can be transported to and from the reaction zone. Studies of the kinetics of such desulphurization reactions have often in the past been complicated by considerations of stirred melts. To gain an insight into the fundamental mechanisms of transport, experiments in the present work have been carried out on unstirred metal/slag systems.

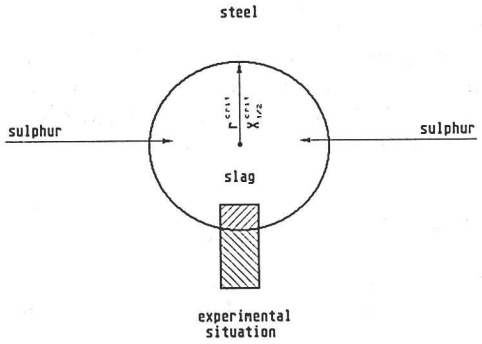

Fig. 1 Suspended slag droplet and experimental simulation

2. Experimental procedure

To simulate suspended slag droplets in practice (figure 1), powder slags of varying compositions (see table 1) were introduced onto the surface of liquid steel samples held in sintered Al_2O_3 crucibles, which were located in the constant temperature zone of a gas-tight Tammann furnace, previously flooded with argon. A perforated graphite disc was served as retainer ring for the crucibles (figure 2). The diameter to height ratio of crucibles was chosen small to suppress any influence of crucible geometry on the concentration profiles recorded.

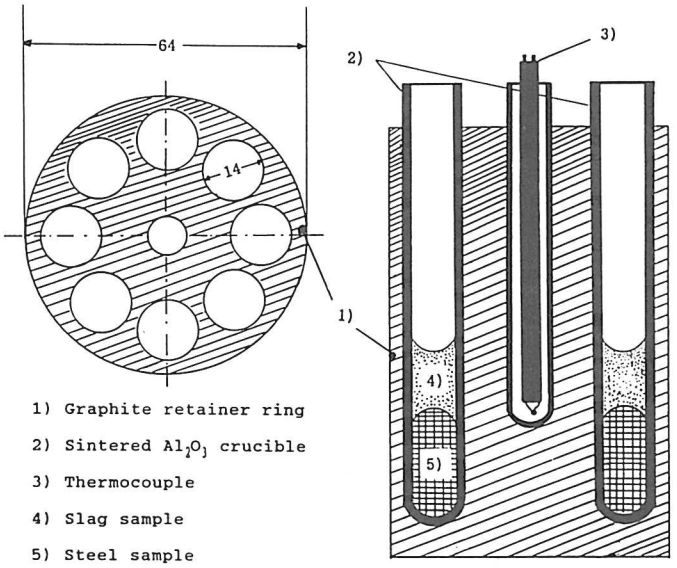

Fig. 2 Perforated graphite disc and crucibles (dimensions in mm)

Table 1: Composition, basicity and viscosity of the slags used
Λ = Optical basicity, ν = Viscosity at 1550°C

No	CaO wt-%	SiO_2 wt-%	Al_2O_3 wt-%	B (CaO)/(SiO_2)	Λ	ν poise
1	42.15	47.85	10	0.88	0.64	14.25
2	46.10	43.90	10	1.05	0.66	9.91
3	48.53	41.47	10	1.17	0.67	3.06

After melting of the steel samples, which contained initial sulphur contents of 0.036%, 0.067% and 0.11% , the slag powder was added at prescribed intervals. Allowing for a melting time of 30 seconds, this gave reaction times of 2, 6, 11 and 16 minutes. The samples were then rapidly cooled under argon flow, and the sulphur and iron profiles determined by microprobe analysis.

Table 2: Compositions of the steels used

No	C %	Si %	Mn %	P %	S %	Al %	Cr %	H ppm	N ppm	O ppm
1	0.35	0.23	0.182	0.022	0.036	0.011	0.092	6.7	34	51
2	0.35	0.23	0.182	0.022	0.067	0.011	0.092	7.2	30	49
3	0.35	0.23	0.182	0.022	0.110	0.011	0.092	6.6	29	50

3. Results and discussions

The sulphur concentration in the steel melt [S] and in the slag (S) are in general dependent on both time and place, as indicated in equation 4 of the appendix. Figures 3.1 and 3.2 show the concentration profile fits of sulphur and iron for an acid (B=0.88) and a basic slag (B=1.17). There is a striking difference in iron and sulphur profiles between the two slags.

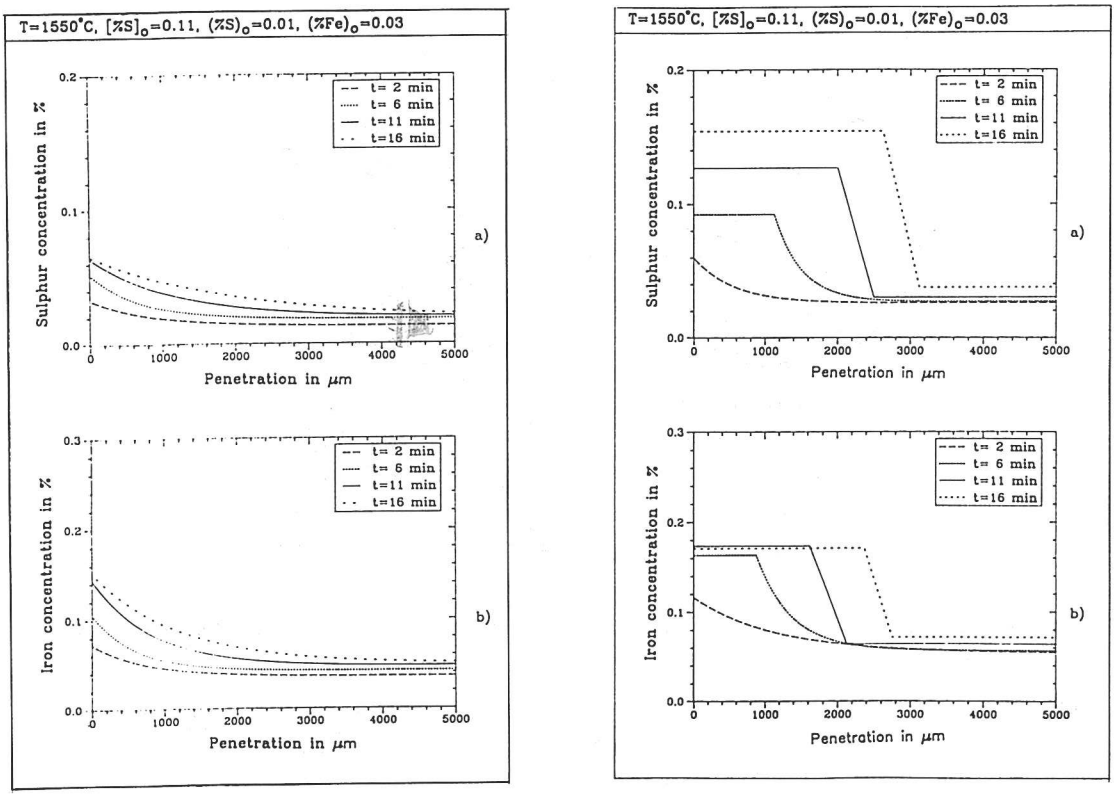

Fig. 3.1 and 3.2 Concentration profiles of sulphur and iron for an acid slag B=0.88 (left) and a basic slag B=1.17 (right)

The acid slag shows a parabolic profile, whereas there is a clearly stepwise pattern for the basic slag, with the exception of the 2 minute reaction time. Also, it can be seen that both iron and sulphur are transported in a similar manner. This, however, will be dealt with in a subsequent paper. A general picture of the profile patterns in basic slags is shown in figure 4, where three distinct zones are evident. Zone 1 covers the transport within the steel melt, zone 2 boundary convection within the slag near the phase boundary, and zone 3 the predominantly diffusion governed slag phase.

Sulphur profiles in zones 1 and 3 (diffusion zones): Both zones exhibit transport via simple diffusion. The sulphur concentrations follow the solution of the general diffusion equations [1,2,3], as indicated in equations 5 and 6 of the appendix. This also is valid for the reaction time of 2 minutes in the basic slag.

Sulphur profiles in zone 2 (convection zone): Above a critical sulphur content of (S) = 0.06 %, as measured in basic slags at the slag/metal boundary, the profile takes on a characteristic stepwise pattern, i.e. transport is by convection. Below this critical value the convection zone in effect does not exist. In general, both diffusion and convection play a role in zone 2, with convection as the dominant factor. This convection, also referred to as boundary convection, produces pronounced mixing in the slag and a levelling effect on the sulphur content to an almost constant value in this zone. The lowering of the interfacial tension between steel and slag with increasing sulphur content in the slag [4,5] may be a contributory cause of this convection. The increase in sulphur concentration $(S)^*$ at the phase boundary with time in zone 2 can be described by:

$$(S)^* = a(1-e^{-bt}) + (S)_0 \qquad (1)$$

where a is the difference between the equilibrium and initial sulphur values and b the sulphur absorption rate. Both constants depend on experimental conditions, in particular on the basicity B = $(CaO)/(SiO_2)$ and $[S]_0$, the initial sulphur content of the steel.

Definition of a characteristic penetration depth: Defining a characteristic penetration depth in terms of the concentration drop to be half of the phase boundary value (see figure 4) leads to the general relationship:

$$X_{\frac{1}{2}} = d \cdot \sqrt{t} \qquad (2)$$

with d as rate of penetration ($mm/sec^{1/2}$). The thus defined half concentration value $X_{1/2}$ can be applied equally to a parabolic profile.

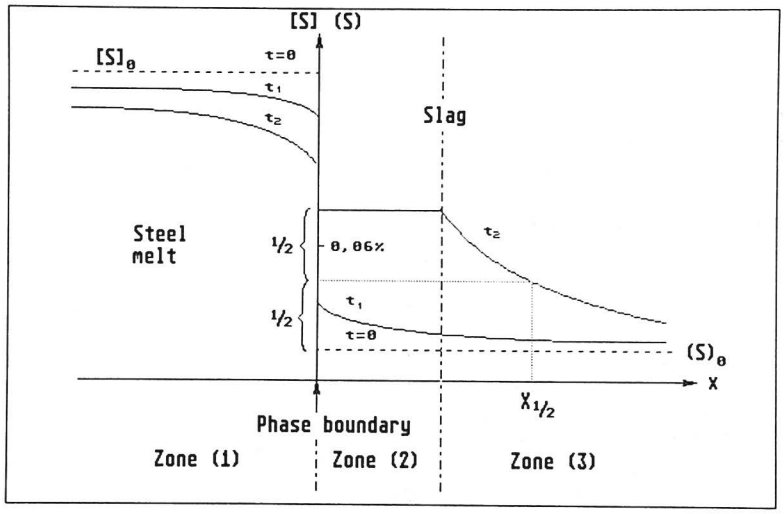

Fig. 4 Schematic plot of sulphur concentration in basic slags

Table 3 gives the experimental values of a, b and d. The reciprocal of "2b" represents a characteristic time scale τ, which is the time needed to reach the peak of maximum sulphur pick-up for a droplet.

Table 3: Experimental values for the parameters a,b and d

B = CaO/SiO_2	$[S]_0$ [%]	a [%]	b [sec^{-1}]	d [$mm/sec^{1/2}$]	τ [min]
0.88	0.110	0.0566	0.0040	0.034	2.1
1.05	0.110	0.0866	0.0034	0.059	2.5
	0.067	0.0576	0.0046	0.040	1.8
	0.036	0.0286	0.0104	0.020	0.8
1.17	0.110	0.1572	0.00191	0.088	4.4

Determination of critical droplet radius For effective desulphurization in practice it is important to obtain the maximum desulphurization rate within a short time span. By combining the experimentally determined half concentration value $X_{1/2}$ with the relevant sulphur content, it is possible to define a critical slag drop radius for attaining maximum sulphur pick-up under a given set of conditions. A mathematical description of the method is given in the appendix, which in essence consists in establishing the point of inflection on the sulphur concentration/half value curve (figure 5). This in turn gives the maximum between accelerated and decelerated sulphur pick-up (figure 6). The points in figure 5 correspond to the half value points in figure 3.2 (upper), with the exception of the time interval of 2 minutes.

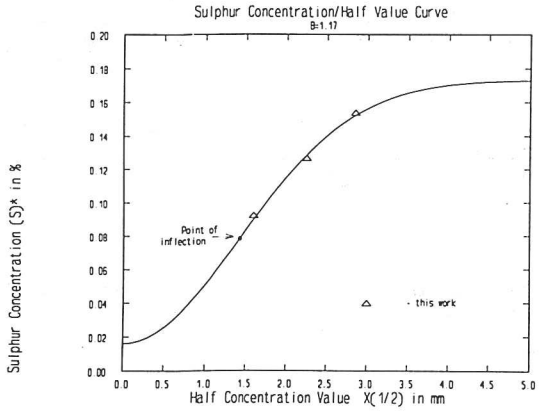

Fig. 5 The sulphur concentration/ half value curve, $(S)^*$ = phase boundary concentration

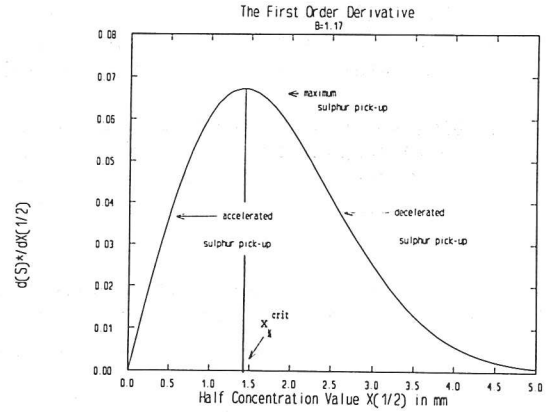

Fig. 6 The first order derivative of the sulphur concentration/ half value curve

The critical droplet radius is given by:

$$r^{crit} = X_{\frac{1}{2}}^{crit} = \frac{d}{\sqrt{2 \cdot b}} \qquad (3).$$

For radii less or greater than r^{crit} desulphurization is accelerated or decelerated respectively. Figure 7 gives this radius as a function of slag basicity, and figure 8 as a function of initial sulphur content in the steel. Of particular interest is the effect of slag basicity combined with the droplet size. This shows that with basic slags a better utilization of slag is possible, since a larger droplet size will be capable of absorbing more sulphur before the critical desulphurizing point has been exceeded.

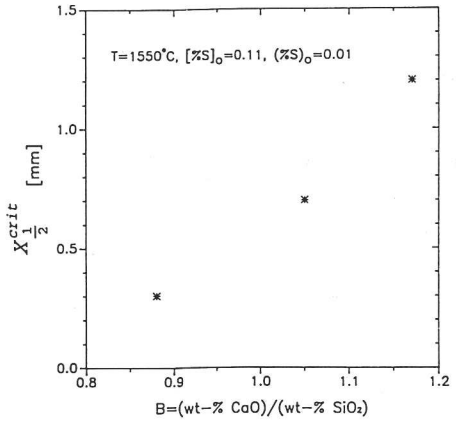

Fig. 7 Influence of slag basicity on the critical radius ($X_{1/2}^{crit}$) of slag droplet

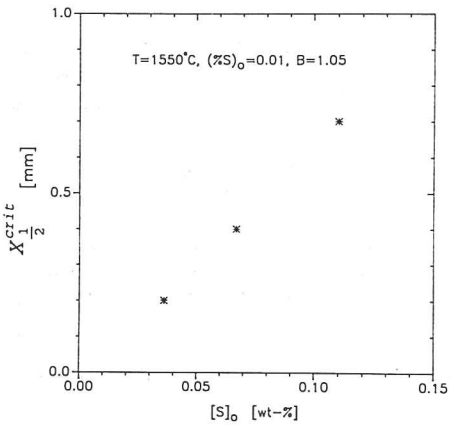

Fig. 8 Influence of initial sulphur content in the steel on the critical droplet radius ($X_{1/2}^{crit}$)

Acknowledgement

The authors would like to thank the Deutsche Forschungsgemeinschaft (DFG) for funding this work.

APPENDIX

Sulphur concentrations S, (S) or [S] as a function of time and place can be expressed by the partial differential equation (4), which in its general

form takes into account diffusion, convection and chemical reaction [6,7].

$$\frac{\partial S}{\partial t} = \nabla(D\cdot\nabla S) - \nabla(\bar{u}\cdot S) - \lambda S \qquad (4)$$

with D the diffusion coefficient, $\bar{u}$ the vectorial velocity of convection flow and λ the rate of chemical reaction. Assuming constant diffusion coefficient D and neglecting convection and chemical reaction, this equation reduces to the differential equation of Fick's second law:

$$\frac{\partial S}{\partial t} = D \cdot \frac{\partial^2 S}{\partial x^2} \qquad (5)$$

where t represents time and x distance. The sulphur concentration in this case is derived from the solutions given in the literature [1,2,3]:

$$S = constant \cdot erfc\left(\frac{x}{2\sqrt{Dt}}\right) \qquad (6)$$

To determine the critical radius of a suspended slag droplet, eliminate time t in the equilibrium concentration $(S)^*$ at the phase boundary of zone 2 to obtain the relation between $(S)^*$ and the half concentration value $X_{1/2}$, thus:

$$(S)^* = a\cdot\left(1-e^{-b\cdot\left(\frac{X_{1/2}}{d}\right)^2}\right) + (S)_0 \qquad (7)$$

The first and second order derivatives of this equation give:

$$\frac{\partial (S)^*}{\partial X_{1/2}} = \frac{2\cdot a\cdot b}{d^2}\cdot X_{1/2}\cdot e^{-b\cdot\left(\frac{X_{1/2}}{d}\right)^2} \qquad (8)$$

$$\frac{\partial^2 (S)^*}{\partial X_{1/2}^2} = \frac{2\cdot a\cdot b}{d^2}\cdot\left(1-\frac{2\cdot b}{d^2}X_{1/2}^2\right)\cdot e^{-b\cdot\left(\frac{X_{1/2}}{d}\right)^2} \qquad (9).$$

The first equation describes the change $d(S)^*$ in the equilibrium concentration from $(S)^*$ to $(S)^* + d(S)^*$ by an increase in half value of $X_{1/2}$ to $X_{1/2}+dX_{1/2}$. The biggest increase is then given by the maximum of $d(S)^*/dX_{1/2}$. Therefore to define the critical droplet radius take either the maximum of the first derivative or the passage through zero of the second derivative:

$$r^{crit} = X_{\frac{1}{2}}^{crit} = \frac{d}{\sqrt{2\cdot b}} \qquad (10)$$

REFERENCES

1] G. Astarita: "Mass Transfer with Chemical Reaction"
Elsevier Publishing Company, Amsterdam/London/New York 1967

2] J. Crank: "The Mathematics of Diffusion"
Oxford University Press, Oxford 1967

3] W. Jost and K. Hauffe: "Diffusion"
Dr. Dietrich Steinkopff Verlag, Darmstadt 1972

4] R. Brückner: Interfacial Convection under Reduced Gravity
in: "Flüssigkeitsgrenzflächen und Benetzung"
Workshop Battelle-Inst. e.V., Frankfurt/M, June 1981, p. 68

5] H. Oertel and K.R. Kirchartz: "Theoretische und experimentelle
Untersuchungen der Zellularkonvektion... " BMFT-Forschungsbericht, 1979

6] R.B. Bird, W.E. Stewart and E.N. Lightfoot:
"Transport Phenomena" John Wiley & Sons, 1960

7] R.S. Brodkey and H.C. Hershey: "Transport Phenomena,
A Unified Approach" , Mc Graw-Hill Book Company, 1989